ISSN (Print) 1226-1750
ISSN (Online) 2233-6656
Journal of Magnetics 18(3), 221-224 (2013) http://dx.doi.org/10.4283/JMAG.2013.18.3.221

Temperature Dependence of Mn^{2+} Paramagnetic Ion in a Stoichiometric $LiNbO_3$ Single Crystal

Tae Ho Yeom* and Soo Hyung Lee

Department of Laser and Optical Information Engineering, Cheongju University, Cheongju 360-764, Korea

(Received 2 May 2013, Received in final form 18 June 2013, Accepted 24 June 2013)

Electron paramagnetic resonance (EPR) spectra of Mn^{2+} impurity ion in Stoichiometric $LiNbO_3$ single crystal (SLN) was investigated with an X-band EPR spectrometer in the temperature range of 3 K~296 K. The intensity of EPR spectrum of Mn^{2+} ion was increased to 20 K and decreased again below 20 K as the temperature decreases. The zero-field splitting parameter D decreased as the temperature increases. It was suggested that Mn^{2+} ion substitute for Nb^{5+} ion instead of Li^+ ion. No changes for hyperfine interaction of Mn^{2+} ion was obtained in the temperature range of 3 K~296 K.

Keywords: $LiNbO_3$ single crystal, Mn^{2+} ion, electron paramagnetic resonance, temperature dependence

1. Introduction

Lithium niobate ($LiNbO_3$) is a typical non-stoichiometric material, and is usually grown by the Czochralski method from a congruent melt. $LiNbO_3$ single crystal has been widely used due to its ferroelectric, piezoelectric, photoelectric properties, holographic volume storage, coherent optical amplification, and phase conjugation [1-7]. However, the congruent $LiNbO_3$ (CLN) crystals used usually contained a considerably large amount of intrinsic defects due to Li deficiency, which lead to the long response times, low refractive index changes and low sensitivities. These large amounts of intrinsic defect greatly degrades the applications of $LiNbO_3$ crystals [8, 9].

The photorefractive properties of un-doped CLN crystals are often relatively poor. $LiNbO_3$ crystals doped with transition metal ion Cu, Fe, Mn, Ce etc., exhibit significant photorefractive properties and are potential material for holographic memories [10-12]. The photorefractive effect, which is used for the storage of volume phase holograms, is due to the presence of transition metal impurities and intrinsic lattice defects [13]. Both the photorefractivity and quality of holography depend on the presence of defects generated during growth as well as deliberately added impurities, usually the transition metal ions. The incorporation of active ions allows the fabrication of photonic devices such as integrated lasers and amplifiers [14]. Doping with damage-resistant dopants is also found to be an effective method that increases the optical damage resistance [15].

Recently, the stoichiometric $LiNbO_3$ (SLN) crystal has attracted much attention for its improvements in many physical properties as compared with CLN crystal [16-20]. The SLN crystals show larger electro-optical and nonlinear effects than those of the CLN crystals [21]. In addition, the coercive fields of the SLN crystals have been reported to be much lower, approximately one-fifth of the CLN crystals at room temperature [22]. Increasing the [Li]/[Nb] ratio in $LiNbO_3$ can also reduce the intrinsic defect concentrations greatly, and thus, the response time can be shortened to the order of seconds in stoichiometric crystals [23].

Since the impurity and defect can strongly influence the electric, optical and magnetic properties of $LiNbO_3$ crystal, the spectroscopy studies of $LiNbO_3$ including impurity and defect have gained considerable interests [24-27]. The local site symmetry, the substituted position and ionic state of the optically active ions in $LiNbO_3$ crystal can be determined by EPR techniques [28]. A number of NMR [29] and EPR [30-33] studies have been performed on Mn^{2+} doped $LiNbO_3$ crystals. In this study, the EPR study of Mn^{2+} ion in stoichiometric $LiNbO_3$ single crystal has been investigated as a function of temperature. The temperature dependence of zero-field splitting parameter and

*Corresponding author: Tel: +82-43-229-8555
Fax: +82-43-229-8432, e-mail: thyeom@cju.ac.kr

intensity of Mn^{2+} spectra are analyzed to find the substituted site location of Mn^{2+} impurity ion in the host material.

2. Crystal Structure and Experiments

The unit cell of $LiNbO_3$ is rhombohedral with the lattice constants at room temperature, a = 0.514739 nm and c = 1.385614 nm [34]. The space group of $LiNbO_3$ belongs to R3c (C_{3v}^6) [35]. The $LiNbO_3$ structure is build of oxygen atoms arranged in planar sheets which form chains of trigonally distorted octahedral, adjoined by walls, spreading along the crystallographic c-axis. The sequence of octahedral repeats [Nb, vacancy, Li] along the c-axis, so 1/3 amount of the octahedral is empty [34, 35].

The impurity ions may occupy one of the three octahedral sites (Nb^{5+}, vacant octahedron, Li^+). The $LiNbO_3$ contains several defects including anti-site defects (Nb^{5+} ion in a Li^+ site, namely Nb_{Li}) and three octahedral sites. All paramagnetic sites positioned along the c-axis of $LiNbO_3$ crystal have the C_3 point group symmetry, while the impurity ions at other positions have the lowest C_1 symmetry [36].

An X-band Jeol EPR spectrometer was employed to record the Mn^{2+} spectra in SLN single crystal. Fig. 1 shows a typical EPR spectrum of Mn^{2+} ion at room temperature when magnetic field B is applied to the crystallographic c-axis. The five groups of lines labeled 1, 2, 3, 4, 5 are the fine structures of Mn^{2+} (S = 5/2), and the six lines within each group are the hyperfine structures of ^{55}Mn (I = 5/2, 100% abundance).

To examine the temperature dependence of EPR parameters for the Mn^{2+} ion in a SLN single crystal, the resonance spectra were measured at different temperatures in the range 3~296 K. Fig. 2 shows the temperature

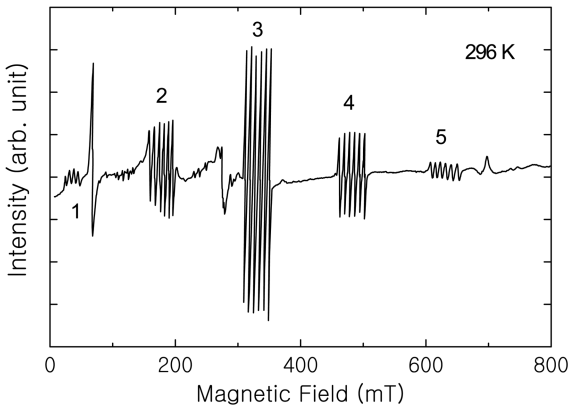

Fig. 1. Typical EPR spectra of Mn^{2+} ion in stoichiometric $LiNbO_3$ single crystal when magnetic field B is applied to the crystallographic c-axis.

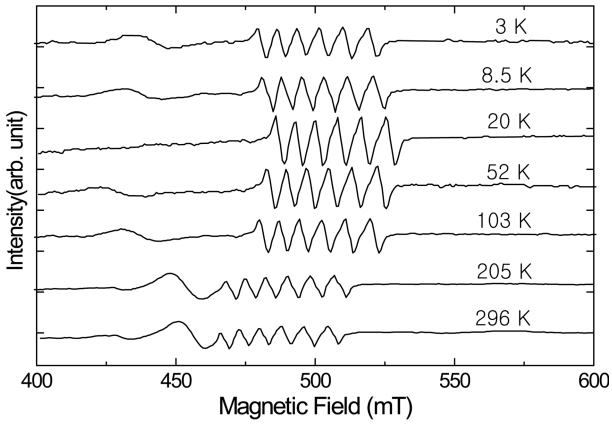

Fig. 2. Temperature dependence of Mn^{2+} ion in stoichiometric $LiNbO_3$ single crystal when magnetic field B is applied to the crystallographic a-axis.

dependence of Mn^{2+} ion at seven different temperatures when magnetic field B is applied to the crystallographic a-axis. The peak-to-peak intensity of Mn^{2+} EPR lines increases approximately linearly with decreasing temperatures from RT to 20 K and reaches a maximum at a temperature of 20 K. Below the 20 K, however, the peak-to-peak intensity decreases.

3. Analysis

The Mn^{2+} ion has the electron configuration $3d^5$ and is an S-state ion with S = 5/2 and a basic level of $^6S_{5/2}$. When this ion is embedded in a SLN crystal, it experiences an intense crystal field produced by the neighboring ions because the 3d shell of the Mn^{2+} ion is the outmost one. Consequently, fine structure arises from the crystal field, and the spin-spin interaction and the hyperfine structure results from the interaction between the nuclear spin of ^{55}Mn and its electronic spin. Accordingly, the experimental results for the resonance fields can be analyzed with the usual spin Hamiltonian [37]

$$H = H_Z + H_{zfs} + H_h \tag{1}$$

where the terms on the right-hand side are the Zeeman interaction, the fine structure (zero-field splitting) and the hyperfine interaction, respectively. The Zero-field splitting term is

$$H_{zfs} = \Sigma B_k^q O_k^q \tag{2}$$

where O_k^q is the extended Stevense operators [38]. The relation between the conventional and Stevense notations is $D = 3B_2^0$ [37]. The hyperfine interaction is

$$H_h = \boldsymbol{S \cdot A \cdot I} \tag{3}$$

where $\boldsymbol{A}$ represents the hyperfine tensor. $\boldsymbol{S}$ and $\boldsymbol{I}$ are the electron and nuclear spin vectors, respectively.

The peak-to-peak intensity of Mn^{2+} EPR line increases almost linearly with decreasing temperatures from RT to 20 K as can be seen Figure 2. When an external magnetic field is applied, magnetization is inversely proportional to the temperature from the Curie law. Therefore, it is reasonable that the intensity of resonance line for Mn^{2+} paramagnetic impurity ion increases as the temperature decreases because magnetic moments of Mn^{2+} ion seem to align as the temperature decreases. However, the intensity of Mn^{2+} EPR line reaches a maximum at a temperature of 20 K and decreases below the 20 K. It seems that the alignments of magnetic moments of Mn^{2+} ion is frustrated under 20 K. Therefore, the intensity of Mn^{2+} resonance line decreases below 20 K. The geometrical magnetic frustrations are studied in amorphous materials, glasses, or dilute magnets, which is a state exhibiting magnetic frustration at low temperatures. The Ho-, Dy-, and Gd-based double perovskites show the characteristics of geometric magnetic frustration at low temperatures [39].

The ZFS parameter D of Mn^{2+} center can be calculated from the effective spin Hamiltonian Eqs. (1) and (2). The D value was already calculated in many previous papers [30-33]. Only the variation of D values as a function of temperature for Mn^{2+} ion is interested in this study. It is found that the D value decreases as the temperature increases above 20 K which can be easily seen in Fig. 2.

The crystal field is proportional to the nuclear quadrupole coupling constant e^2qQ/h [40]. The ZFS can be changed according to the crystal field. Thus, it may acceptable that ZFS parameter D is proportional to e^2qQ/h when there is some proportionality between CF and ZFS. There is also formal similarity, not physical similarity, between D and e^2qQ/h in EPR and nuclear magnetic resonance (NMR) Hamiltonian [41]. Since Mn^{2+} is spherically symmetric, the electric field gradient (EFG) is directly related to the crystal field parameter [42]. According to the previous EPR measurements, Mn^{2+} ion is located at the site of crystallographic C_3-axis [33]. As the temperature increases, the e^2qQ/h of Li^+ in $LiNbO_3$ increases, whereas e^2qQ/h of Nb^{5+} and D of Mn^{2+} decrease. As the temperature increases, the Nb ions move to the center direction of the inversion so as to occupy a position between the oxygen layers; on the other hand, the Li ions move away from the center of inversion so as to occupy a position in the plane of oxygen layers. When considering the axial components, the crystal field action on the Nb^{5+} decreases and increases at the Li site (if the nearest oxygen ions are considered) [30]. Therefore, from the comparison of temperature dependence between e^2qQ/h and D, we can conclude that Mn^{2+} impurity ion replaces Nb^{5+} ion instead of Li^+ ion in SLN.

The hyperfine interaction of Mn^{2+} paramagnetic impurity ion is obtained from the effective spin Hamiltonian Eqs. (1) and (3). The hyperfine constant $|A|$ was obtained by a first-order perturbation to the Zeeman term because the hyperfine interaction turns out to be much smaller than the Zeeman. The hyperfine constant of Mn^{2+} ion was found to be $|A| = 78.5\ \text{G} \pm 1.5\ \text{G}$ which is constant within experimental accuracy of the temperature range 3~296 K.

4. Results

The temperature dependence of Mn^{2+} paramagnetic impurity ion in stoichiometric $LiNbO_3$ single crystal has been investigated by EPR spectrometer. The peak-to-peak intensity of Mn^{2+} resonance line increases as the temperature decreases which is consistent with Curie law. The intensity of Mn^{2+} paramagnetic ion was decreased from the magnetic frustration at low temperatures. The zero-field splitting parameter decreases as the temperature increases. It was suggested that the Mn^{2+} impurity ion substitutes for the Nb^{5+} ion instead of Li^+ ion in stoichiometric $LiNbO_3$ single crystal when comparing the temperature dependences between the ZFS parameter and crystal field. The hyperfine splitting of Mn^{2+} ion in SLN does not change as the temperature changes from 3~296 K.

References

[1] I. Tomeno and S. Matsumura, J. Phys. Soc. Japan **56**, 163 (1987).
[2] K. Buse, F. Jermann, and E. Kratzig, Opt. Matter. **4**, 237 (1995).
[3] D. K. McMillen, T. D. Hudson, J. Wagner, and J. Singleton, Opt. Express **2**, 491 (1998).
[4] J. Imbrock, S,. Wevering, K. Buse, and E. Kratzig, J. Opt. Soc. Am. B **16**, 1392 (1999).
[5] X. Yue, A. Adibi, T. Hudson, K. Buse, and D. Psaltis, J. Appl. Phys. **87**, 4051 (2000).
[6] T. Pliska, D. Fluck, and P. Gunter, in Nonlinear Optical Effects and Materials, edited by P. Gunter, Springer, Berlin (2000) pp. 479-482.
[7] T. Hatanaka, K. Nakamura, T. Taniuchi, H. Ito, Y. Furukawa, and K. Kitamura, Opt. Lett. **25**, 651 (2000).
[8] R. L. Byer and J. F. Young, J. Appl. Phys. **41**, 2320 (1970).
[9] S. Kostritskii and O. Sevostyanov, Appl. Phys. B **65**, 527 (1997).
[10] M. Ohira, Z. Chen, and T. Kasanmatsu, Jpn. J. Appl. Phys. **30**, 2326 (1991).
[11] T. Tsuboi, M. Grinberg, and S. M. Kaczmarek, J. Alloys

Compd. **341**, 333 (2002).
[12] Y. Yang, D. Psaltis, M. Luennemann, D. Berben, U. Hartwig, and K. Buse, J. Opt. Soc. Am. B **20**, 1491 (2003).
[13] K. Buse, F. Jermann, and E. Kratzig, Appl. Phys. A **58**, 191 (1994).
[14] E. Cantelar, J. A. Sanz-Garcia, G. Lifante, F. Cusso, and P. L. Pernas, Appl. Phys. Lett. **86**, 161119 (2005).
[15] G. Q. Zhang, G. Y. Zhang, S. M. Liu, J. J. Xu, and Q. Sun, J. Appl. Phys. **83**, 4392 (1998).
[16] Y. Furukawa, K. Kitamura, Y. Ji, G. Montemezzani, M. Zgonik, C. Medrano, and P. Gunter, Opt. Lett. **22**, 501 (1997).
[17] F. Abdi, M. Aillerie, P. Bourson, M. D. Fontana, and K. Polgar, J. Appl. Phys. **84**, 2251 (1998).
[18] Y. Furukawa, K. Kitamura, K. Niwa, and H. Hatano, Opt. Lett. **23**, 1892 (1998).
[19] T. Zhang, B. Wang, S. Fang, and D. Ma, J. Phys. D: Appl. Phys. **38**, 2013 (2005).
[20] Z. Xu and Y. Xu, Mater. Lett. **61**, 3243 (2007).
[21] T. Fujiwara, M. Takahashi, M. Ohama, A. Ikushima, Y. Furukawa, and K. Kitamura, Electron. Lett. **35**, 499 (1999).
[22] V. Gopalan, T. Mitchell, Y. Furukawa, and K. Kitamura, Appl. Phys. Lett. **72**, 1981 (1998).
[23] X. Chen, D. Zhu, B. Li, T. Ling, and Z. Wu, Opt. Lett. **26**, 998 (2001).
[24] O. F. Schirmer, O. Thiemann, and M. Wohlecke, J. Phys. Chem. Solids **52**, 185 (1991).
[25] T. H. Yeom, S. H. Choh, Y. M. Chang, and C. Rudowicz, Phys. Stat. Sol. (b) **185**, 409 (1994).
[26] T. H. Yeom, S. H. Lee, S. H. Choh, and D. Choi, J. Korean Phys. Soc. **32**, S647 (1998).
[27] V. Grachev and G. Malovichko, Phys. Rev. B **62**, 7779 (2000).
[28] S. H. Lee, T. H. Yeom, and S. H. Kim, J. Magnetics **17**, 251 (2012).
[29] H. W. Shin, S. H. Choh, T. H. Yeom, and K. S. Hong, J. Korean Phys. Soc. **32**, S662 (1998).
[30] M. P. Petrov, Soviet Phys.-Solid State **10**, 2574 (1969).
[31] D. G. Rexford and Y. M. Kim, J. Chem. Phys. **57**, 3094 (1972).
[32] M. D. Glinchuk, G. I. Malovichko, I. P. Bykov, and V. G. Grachev, Ferroelectrics **92**, 83 (1989).
[33] T. H. Yeom, S. H. Choh, Y. M. Chang, and C. Rudowicz, Phys. Stat. Sol. (b) **185**, 417 (1994).
[34] S. C. Abrahams and P. Marsh, Acta Cryst. B **42**, 61 (1986).
[35] S. C. Abrahams, J. M. Reddy, and J. L. Bernstein, J. Phys. Chem. Solids **27**, 997 (1966).
[36] G. Malovichko, V. Grachev, V. Kokanyan, and O. Shirmer, Phys. Rev. B **59**, 9113 (1999).
[37] A. Abragam and B. Bleaney, Electron Paramagnetic Resonance of Transition Ions, Oxford University Press, Oxford (1970).
[38] C. Rudowicz, Mag. Res. Rev. **13**, 1 (1987).
[39] H. Karunadasa, Q. Huang, B. G. Ueland, P. Schiffer, and R. J. Cava, Proceedings of the National Academy of Sciences of the USA **100**, 8097 (2003).
[40] G. Burns, J. Chem. Phys. **31**, 1253 (1959).
[41] S. H. Choh, H. T. Kim, H. K. Choh, C. S. Han, D. Choi, and J. N. Kim, Bull. Mag. Res. **11**, 371 (1989).
[42] W. J. Nicholson and G. Burns, Phys. Rev. **129**, 2490 (1963).